

A Novel Dual-Band Unequal Filtering Power Divider

Yong Xia^{1, *}, Feng Wei², and Xiao-Wei Shi²

Abstract—In this paper, an unequal Filtering Power Divider (FPD) adopting a novel dual-band resonator and inter-digital feeding lines structure is presented. By integrating the resonator and modifying coupling mode, filtering and unequal power distribution are all achieved on the base of the deformed Wilkinson power divider. Two sets of cascading resonators operating at 2.45/4.44G with the same structure are proposed for WIFI and other application. Keeping with the unchanged coupling mode, the unequal ratio of 2 : 1 is arrived by adjusting the strength of coupling. The two resonant frequencies can be adjusted independently to ensure the flexibility of the design. For verifying the theoretical designs and simulated results, a fabricated FPD is exhibited, analyzed, and measured. The simulated results are in good agreement with the measured ones with slight variations.

1. INTRODUCTION

As the fundamental component in the field of RF and antenna arrays, power dividers applying for combining and splitting power attract much attention [1–3]. With regard to the research direction of power divider, realizing multi-functional power dividers embedded with filters is one of them. The research on the power divider with the function of filtering to meet the demand for miniaturization and diversified functions is a hot spot. At the same time, the research from the perspective of unequal division ratio is another way.

Since Wilkinson power divider was proposed for the first time, whose the modification design has been extensively studied. Submitting the $\lambda/4$ transmission line of a conventional Wilkinson power divider with a filter or other components is a common solution [4–6]. Unequal power divider can also be obtained by deforming the Wilkinson power divider.

The design method about generalized Wilkinson power divider is proposed for arbitrary power division and arbitrary-way by changing the transmission line impedance and cascading mode [7]. So, the design of transmission line impedance is the main idea [8]. A Wilkinson power divider with the characteristics of negative group delay (NGD) can be achieved by adjusting the branch-line and terminal impedance resistors [9].

A Wilkinson power divider with high ratio is also the focus of the design. In [10], a 8 : 1 Wilkinson power divider is produced by cascading one 3 : 1 and two 2 : 1 dividers. Higher power division ratios, such as 10 : 1 [11] and 11 : 1 [12] Wilkinson power dividers, are presented by a coupled-line structure and 3-way power divider structure, respectively.

The dynamic adjustment of power division ratio is a promising topic. By tuning the capacitors for achieving the change of the power ratio from 2 : 1 to 3 : 1 or vice versa, an adjustable unequal power divider can be designed by replacing transmission line sections with a T-equivalent circuit [13]. The design adopting lumped-elements is suitable to set arbitrary power division ratio without modifying the design of microstrip [14]. However, it is a deficiency for these design schemes operating at the

Received 12 November 2022, Accepted 3 January 2023, Scheduled 13 January 2023

* Corresponding author: Yong Xia (yxia@stu.xidian.edu.cn).

¹ School of Advanced Materials and Nanotechnology, China. ² School of Electronic Engineering, Xidian University, Xi'an 710071, China.

single-frequency. A wide band unequal FPD can be designed with a ring resonator mounting an open stub and two coupled lines [15]. In [16], an unequal power divider operating at dual bands is proposed, which consists of transmission lines and parallel stubs without reactive components. Power dividers based on microstrip trees and coupling effect are proposed in [17–19].

In this paper, a dual-band FPD operating at 2.45/4.44G with 2 : 1 power division ratio is proposed. A novel resonator with a symmetric structure acting as a filter is the essential part, which is analyzed by odd-even mode analysis methods. The implementation of unequal division is realized by adjusting the width of the feeding lines instead of changing the characteristic impedance of transmission line. More than three transmission zeroes produced by the resonator and coupled structure contribute to the high frequency selectivity. Depending on the current distribution diagram, each resonant frequency point can be designed separately. In different application fields it can be met for achieving the required resonant frequency by changing the length of stub.

2. RESONATOR DESIGN

In this section, the designed Multi-Mode Resonator (MMR) acting as a filter is given and analyzed. The schematic diagram of resonator being symmetrical to the center line is shown in Fig. 1. The proposed resonator is composed by a grounded end stub, four open stubs, and a ring stub. So, it is a proper way to analyze the proposed resonator adopting the odd-even mode method.

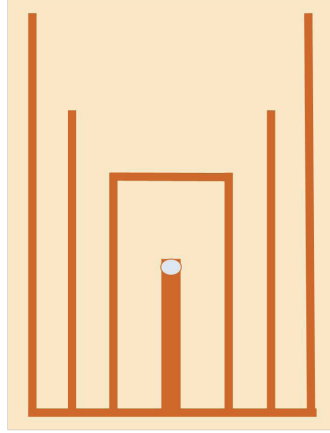


Figure 1. Schematic of the proposed resonator.

The equivalent circuit of even-mode is shown in Fig. 2(a), which comprises three open end stubs and one grounded end stub. The input admittance is given here:

$$Y_{ine} = jY \frac{Y_e + \tan \theta_3 + \tan \theta_2}{1 - (Y_e + \tan \theta_3) \tan \theta_2} + jY \tan \theta_1 \quad (1)$$

$$Y_e = \frac{\tan \theta_4 + \tan \theta_5 - \cot \theta_6}{1 - (\tan \theta_5 - \cot \theta_6) \tan \theta_4} \quad (2)$$

In these formulas, θ_i represents the length of the i th branch, which is defined in (7). The resonant condition is $Y_{ine} = 0$, and the even-mode resonant frequency can be obtained from (3) and (7):

$$\begin{aligned} & \frac{\tan \theta_4 + \tan \theta_5 - \cot \theta_6}{1 - (\tan \theta_5 - \cot \theta_6) \tan \theta_4} + \tan \theta_3 + \tan \theta_2 + \tan \theta_1 \\ & - \tan \theta_1 \left(\frac{\tan \theta_4 + \tan \theta_5 - \cot \theta_6}{1 - (\tan \theta_5 - \cot \theta_6) \tan \theta_4} + \tan \theta_3 \right) \tan \theta_2 = 0 \end{aligned} \quad (3)$$

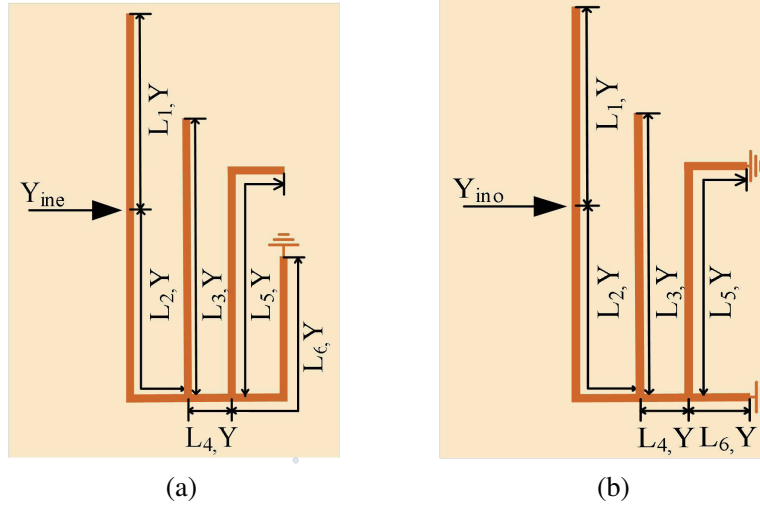


Figure 2. (a) Even-mode equivalent circuit. (b) Odd-mode equivalent circuit.

The equivalent circuit of odd-mode consisting of two grounded end stubs and two open end stubs is shown in Fig. 2(b). The input admittance is given below:

$$Y_{ino} = jY \frac{Y_o + \tan \theta_2}{1 - Y_o \tan \theta_2} + jY \tan \theta_1 \quad (4)$$

$$Y_o = \frac{\tan \theta_4 - \cot \theta_5 - \cot \theta_6}{1 + (\cot \theta_5 + \cot \theta_6) \tan \theta_4} + \tan \theta_3 \quad (5)$$

Similar to the even-mode, the odd-mode resonant condition is $Y_{ino} = 0$. The odd-mode resonant frequent can be obtained from (6) and (7).

$$\frac{\tan \theta_4 - \cot \theta_5 - \cot \theta_6}{1 + (\cot \theta_5 + \cot \theta_6) \tan \theta_4} + \tan \theta_3 + \tan \theta_2 + \tan \theta_1 - \tan \theta_1 \left(\frac{\tan \theta_4 - \cot \theta_5 - \cot \theta_6}{1 + (\cot \theta_5 + \cot \theta_6) \tan \theta_4} + \tan \theta_3 \right) \tan \theta_2 = 0 \quad (6)$$

$$\theta_i = \beta l_i \quad (7)$$

The precise roots of these equations are difficult to calculate for the reason of many variables, and no detailed calculation is necessary. In [6, 20], a similar analysis process and idea are presented.

The odd-mode equivalent circuit cannot be analyzed by odd-even mode method again for its non-symmetrical structure. So, one resonant frequency can be deduced from this equivalent circuit. This even-mode equivalent circuit can be analyzed in the same way. It can be concluded that the proposed resonator can only have two resonant frequencies [5, 6].

The function of the FPD can only be realized by the joint action of the resonator and the feeding line. So, the overall design strategy including the resonators and feeding lines will be analyzed as a whole in next section.

3. FPD DESIGN AND ANALYSIS

The whole design diagram of FPD comprising four resonators, two inter-digital feeding lines of different widths, and two isolation resistors is shown in Fig. 3. On one side of the feeding lines, two resonators proposed in Fig. 1 are cascaded. The widths of two sets of feeding lines are different. Resonators and feeder units constitute the two branches of convention Wilkinson power divider. Adopting the scheme with two isolation resistors is to achieve a better isolation effect.

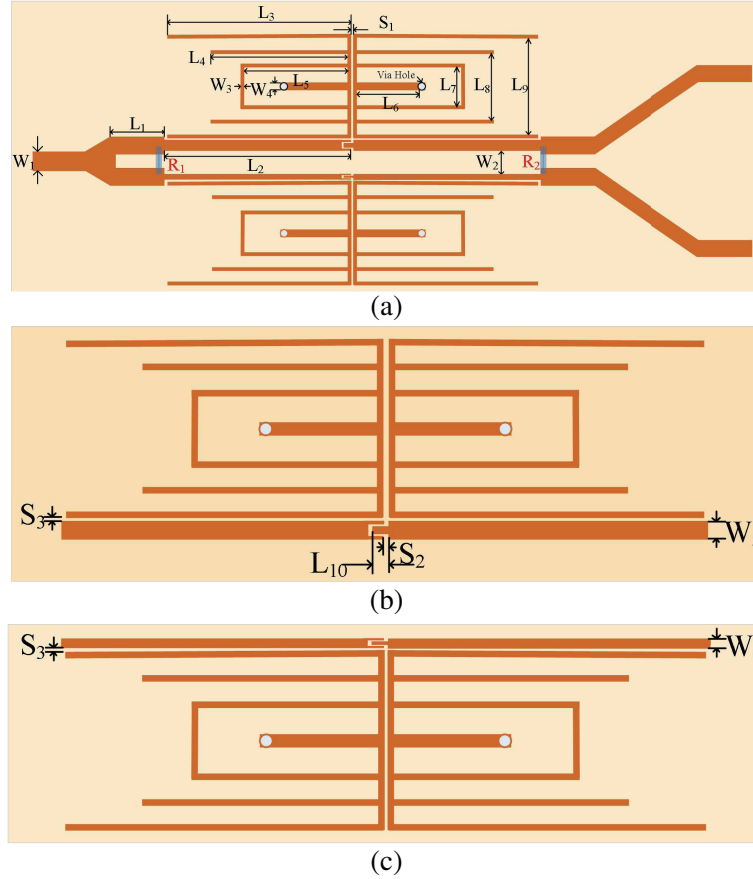


Figure 3. (a) The schematic of dual-mode unequal FPD. (b) The size of top inter-digital coupling lines. (c) The size of bottom inter-digital coupling lines. [$W_1 = 1.8$ mm, $W_2 = 2.125$ mm, $W_3 = 0.25$ mm, $W_4 = 0.5$ mm, $W_5 = 1.15$, $W_6 = 0.5$, $L_1 = 3$ mm, $L_2 = 9.44$ mm, $L_3 = 9.14$ mm, $L_4 = 7$ mm, $L_5 = 5.75$ mm, $L_6 = 4$ mm, $L_7 = 1$ mm, $L_8 = 1.8$ mm, $L_9 = 3$ mm, $L_{10} = 0.65$ mm, $S_1 = 0.1$ mm, $S_2 = 0.12$ mm, $S_3 = 0.1$ mm, $R_1 = 200$ ohm, $R_2 = 200$ ohm, $R_{via} = 0.5$ mm].

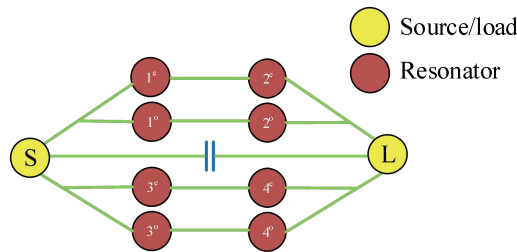


Figure 4. Coupling scheme of the proposed FPD.

The coupling paths of the four resonators and feeding lines are depicted in Fig. 4. The energy can be coupled through the resonator and feeding lines, respectively. Because of the same structure, the cascading resonators below operate at the same resonant frequency as the resonators above.

With the help of the current distribution profile of the FPD, it is easier to adjust the resonant frequency. The diagram that depicts the current distribution of the proposed FPD operating at 2.45G/4.44G is shown in Fig. 5.

According to Fig. 5, only L_6 affects the low resonant frequency while L_3 and L_9 affect the high resonant frequency. The length of L_3 cannot be changed for the design structure.

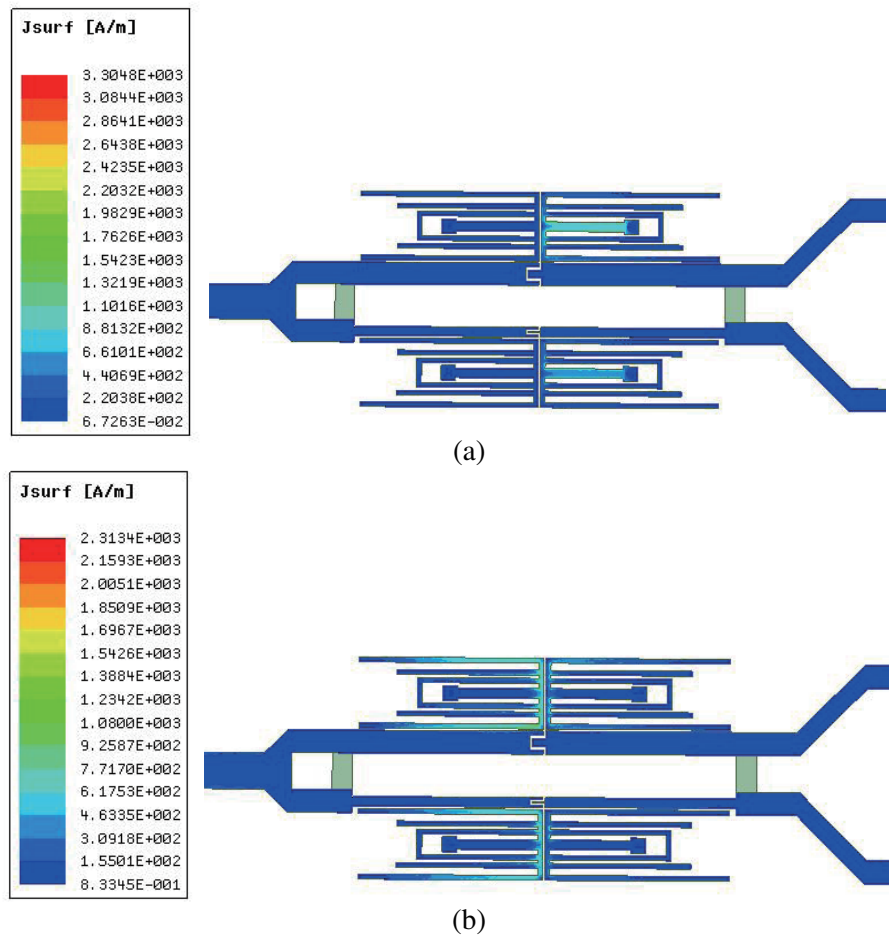


Figure 5. Current distribution of the resonator (a) 2.45G, (b) 4.44G.

In Fig. 6, the relationship between the resonant frequency and the length of microstrip line can be observed easily. The main factor that determines the resonant frequency f_1 is the length of L_6 , not L_9 . The length of L_9 has a big effect on f_2 and a small effect on f_1 . Independently adjust the two resonant frequencies in two steps. The researchers determine f_2 by adjusting the length of L_9 for completing the first step, then, make the length adjustment of L_6 for f_1 . Here, the fact that two resonant frequent points may be adjusted independently can help researchers design various FPDs for different purposes.

4. SIMULATED AND MEASURED RESULTS

In this section, the measured results will be given for comparing and judging the feasibility of the scheme further.

A photograph of the material object of FPD is shown in Fig. 7, and it is fabricated using Rogers 4350. The thickness of substrate is 0.508 mm, and the dielectric constant is 3.48. As shown, the overall size is about 26 mm * 36.5 mm, which is tested by Agilent vector network analyzer. From the measured results, the resonance frequency point has only a small deviation in Fig. 8(a), and 2 : 1 power division ratio is obtained in Fig. 8(b) for the reason of 3 dB difference between S_{21} and S_{31} at the resonant frequency. The isolation performance of two output ports is better than 10 dB, which meets the isolation requirements. For fabrication reasons, small deviations exist in the measured results compared with the simulated results.

In Fig. 8(b), the three transmission zeroes generated by inter-digital couplings structure and mixed magnetic and electric couplings induce high frequency selectivity. The sharp skirts of two passbands

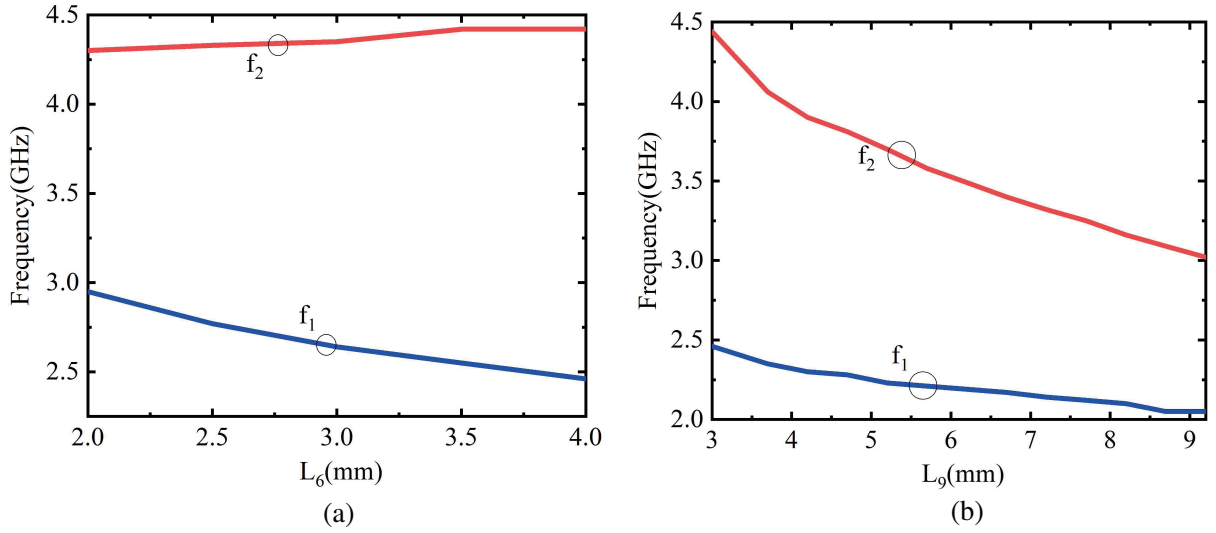


Figure 6. Resonant frequency with varied dimensions (a) L_6 , (b) L_9 .

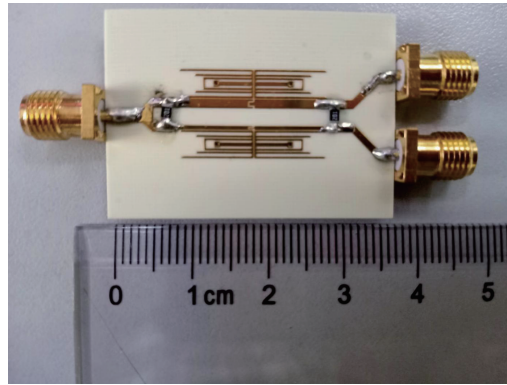


Figure 7. Photograph of the fabricated unequal FPD.

greatly improve the performance of the FPD. With the decrease of L_{10} , the increase of S_2 , and the falling of coupling capacity of source-load, frequency selecting ability becomes worse because TZ_1 and TZ_2 will merge.

The comparison of multiple performance parameters between the proposed FPD and some recent published works is carried out. The results of comparison can be obtained in Table 1. The performance of this scheme is ideal.

Table 1. Comparisons with previous works.

Ref.	CFs (GHz)	Minimum IL (dB)	Iso. (dB)	RL (dB)	Power ratio
7	0.6/2.45	4.5	> 10	> 20	3 : 5 : 1
8	1.0/2.0	5.8	> 15	> 14	1 : 2
13	2.6	4	> 15	> 15	1 : 2
14	0.435	5.1	> 20	> 22	Adj
This work	2.45/4.44	4.2	> 15	> 14	1 : 2

CFs = Center Frequencies, IL = Insertion Loss, Iso. = Isolation, RL = Return Loss, Adj = Adjustable.

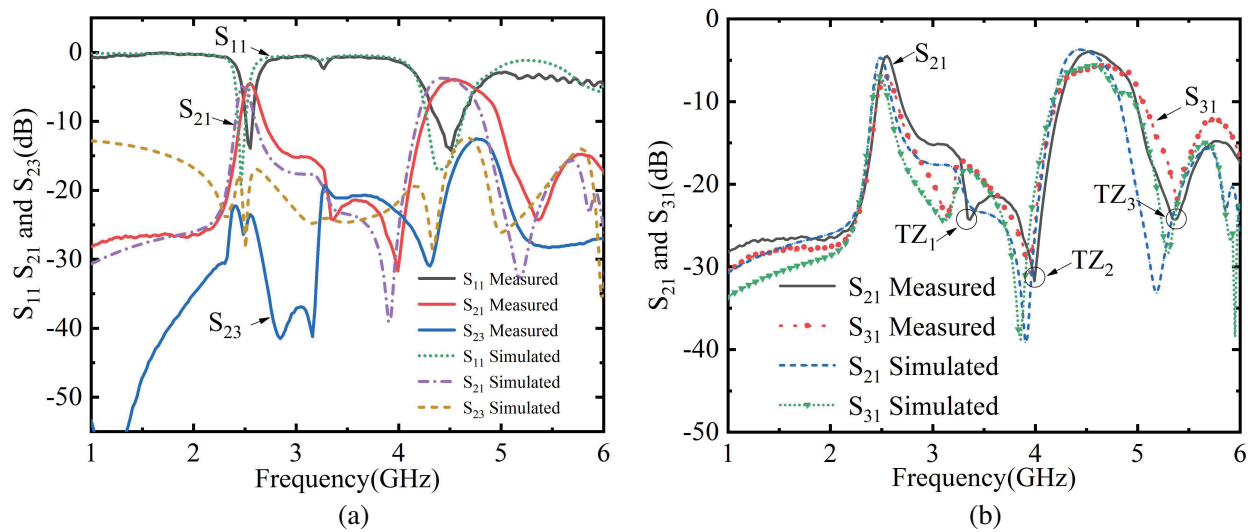


Figure 8. The measured and simulation S-parameters of proposed FPD. (a) S_{11} , S_{21} and S_{23} ; (b) S_{21} and S_{31} .

5. CONCLUSION

The detailed analysis of a novel resonator and the various ways of realizing strength of coupling are carried out, and a dual-band unequal FPD is presented in this paper. The proposed dual-band FPD operating at 2.45/4.44GHz realizes 2 : 1 power division ratio. The measured results of the fabricated FPD has reached a desired level and revealed the validity of design. Good performance of the proposed unequal FPD such as high selectivity and adjustability of center frequency helps to broaden the scope of application.

REFERENCES

1. Abbosh, A. M., "A compact UWB three-way power divider," *IEEE Microw. Wireless Compon. Lett.*, Vol. 17, No. 8, 598–600, Aug. 2007.
2. Park, M.-J. and B. Lee, "A dual-band Wilkinson power divider," *IEEE Microw. Wireless Compon. Lett.*, Vol. 18, No. 2, 85–87, Feb. 2008.
3. Wilkinson, E., "An N-way hybrid power divider," *IRE Trans. Microw. Theory Tech.*, Vol. 8, No. 1, 116–118, Jan. 1960.
4. Li, Y. C., Q. Xue, and Y. X. Zhang, "Single- and dual-band power dividers integrated with bandpass filters," *IEEE Trans. Microw. Theory Tech.*, Vol. 61, No. 1, Jan. 2013.
5. Liu, W. Q., F. Wei, and X. W. Shi, "A compact tri-band power divider based on triple-mode resonator," *Progress In Electromagnetics Research*, Vol. 138, 283–291, 2013.
6. Chen, L. and F. Wei, "Compact quad-band power divider based on quad-mode stub loaded resonator," *IEEE International Conference on Microwave and Millimeter Wave Technology (ICMMT)*, 2016.
7. Wu, Y. L., Y. N. Liu, Q. Xue, S. L. Li, and C. P. Yu, "Analytical design method of multiway dual-band planar power dividers with arbitrary power division," *IEEE Trans. on Microw. Theory and Techn.*, Vol. 58 No. 12, 2010.
8. Wu, Y. L., H. Zhou, Y. X. Zhang, and Y. A. Liu, "An unequal Wilkinson power divider for a frequency and its first harmonic," *IEEE Microw. Wireless Compon. Lett.*, Vol. 18, No. 11, 737–739, Nov. 2008.

9. Chaudhary, G., J. Park, Q. Wang, and Y. Jeong, "A design of unequal power divider with positive and negative group delays," *Proceedings of the 45th European Microwave Conference*, Sep. 2015.
10. Watkins, G., "A 1 : 8 cascaded Wilkinson power divider," *Proceedings of the 44th European Microwave Conference*, Oct. 2014.
11. Li, B., X. D. Wu, and W. Wu, "A 10 : 1 unequal Wilkinson power divider using coupled lines with two shorts," *IEEE Microw. Wireless Compon. Lett.*, Vol. 19, No. 12, 789–791, Mar. 2009.
12. Chen, H. D., T. Y. Zhang, W. Q. Che, and W. J. Feng, "Compact unequal Wilkinson power divider with large power dividing ratio," *Proceedings of the 44th European Microwave Conference*, Oct. 2014.
13. Yang, C. K. and Y. H. Shih, "An adjustable unequal power divider design," *Applied Proceedings of iWEM 2014*, Sapporo, Japan, 2014.
14. Rǘü, A., A. D. Maria, M. Limbach, R. Horn, and A. Reigber, "A 5 way lumped-elements Wilkinson power divider," *Applied 7th European Conference on Antennas and Propagation (EuCAP)*, 2013.
15. Liu, Y., X. Yu, and S. Sun, "Design of a wideband filtering power divider with stub-loaded ring resonator," *Applied Computational Electromagnetics Society Symposium (ACES)*, Sep. 2017.
16. Wu, Y., Y. Liu, Y. Zhang, J. Gao, and H. Zhou, "A dual band unequal Wilkinson power divider without reactive components," *IEEE Trans. Microw. Theory Tech.*, Vol. 57, No. 1, 216–222, Jan. 2009.
17. Ravelo, B., O. Maurice, and S. Lall  ch  re, "Asymmetrical 1 : 2 Y-tree interconnects modelling with Kron-Branin formalism," *Electronics Letters*, Vol. 52, No. 14, 1215–1216, Jul. 2016.
18. Ravelo, B., A. Normand, and F. Vurpillot, "Modelling of interbranch coupled 1 : 2 tree microstrip interconnect," *ACES Journal*, Vol. 33, No. 3, 285–292, Mar. 2018.
19. Ravelo, B., F. Wan, S. Lall  ch  re, and B. Agnus, "Resistive active balanced power divider design with touchstone and Kron's formalism hybrid model," *ACES Journal*, Vol. 33, No. 5, 530–536, May 2018.
20. Gao, L., X. Y. Zhang, B. J. Hu, and Q. Xue, "Novel multi-stub loaded resonators and their applications to various bandpass filters," *IEEE Trans. Microw. Theory Tech.*, Vol. 62, 1162–1172, 2014.